Journal of Machine Engineering, 2026, Vol. 26
ISSN 1895-7595 (Print) ISSN 2391-8071 (Online)

Received*: 19 January 2026* / Accepted: *16 February 2026* / Published online: *23 February 2026*

machining,
FEM modelling,
friction (COF),
AI-assistance

Wit GRZESIK[1*], Helmi ATTIA[2],
Konrad WEGENER[3] , Joel RECH[4],
Marek BALAZINSKI[5]

INTELLIGENT METHODS FOR QUANTIFYING AND DETERMINING FRICTION IN THE CUTTING PROCESS – A REVIEW

In this paper some recently proposed possibilities of integration of AI (Artificial Intelligence) methods with FEM (Finite Element Method)-based modelling in terms of coefficient of friction (COF) prediction are overviewed and discussed. In particular, the implementation of the Grey-Box model and some regression testing methods are discussed. Some results of the integration of Python interface with FEM DEFORM package regarding componential cutting forces and cutting temperature using predicted COF values are given. The results of implementation of different friction models in FEM and SPH (Smoothed Particle Hydrodynamics) simulation packages are compared. A number of different friction models are considered in quantifying friction and predicting tool wear rate. It was documented that both dedicated tribo-tests and advanced ML prediction algorithms increase visibly the simulation accuracy. New trends and future research directions are overviewed.

1. INTRODUCTION

In the cutting process, friction, alongside mechanical, thermal and tribological interactions, is a fundamental physical phenomenon that determines its overall performance and effectiveness due to its influence on energy dissipation and tool wear [1]. In recent decades, significant progress has been made in the development of measurement methods and techniques aimed at identifying friction not only in quantitative terms, but also in terms of the physical/tribological mechanisms that accompany it under various thermo-mechanical conditions [1, 2, 3, 4]. Previous references [4] for process modelling should be validated and

[1] Manufacturing and Materials Engineering (former), Opole University of Technology (former), Poland
[2] McGill University, Montréal, Canada
[3] Inspire-iwf Werkzeugmaschinen und Fertigung, Zürich, Switzerland
[4] Centrale Lyon ENISE, Saint-Etienne, France
[5] Polytechnique Montréal, Canada
[*] E-mail: wge103@wp.pl
https://doi.org/10.36897/jme/218157

possibly updated due to significant progress in AI-based support. The designs of friction testing devices, the so-called tribometers, were previously described in Refs. [2] and [3] as a result of the Polish-French scientific cooperation and recently re-edited Ref. [5].

In general, the characterization of friction behaviour in the secondary shear zone and in the rubbing zone (see the left upper detail in Fig. 1a) is based on three different methods [2, 3, 5-8]:

- measurements of the components of the resultant cutting force using piezo- or strain-gauge dynamometers (1st type),
- conventional tribometers (2nd type) which are typically used for evaluating the friction coefficient of structural materials, e.g. hard alloys and bearing steels. Unfortunately, this type of tribometers, e.g., pin-on-disc, does not simulate the severe tribological conditions of a heavily loaded system with varying sliding velocities and normal pressures, which are encountered at the tool-work interface.
- specially-designed tribometers (3rd type) which are better adopted for the mechanical, thermal and tribological conditions in the cutting zone.

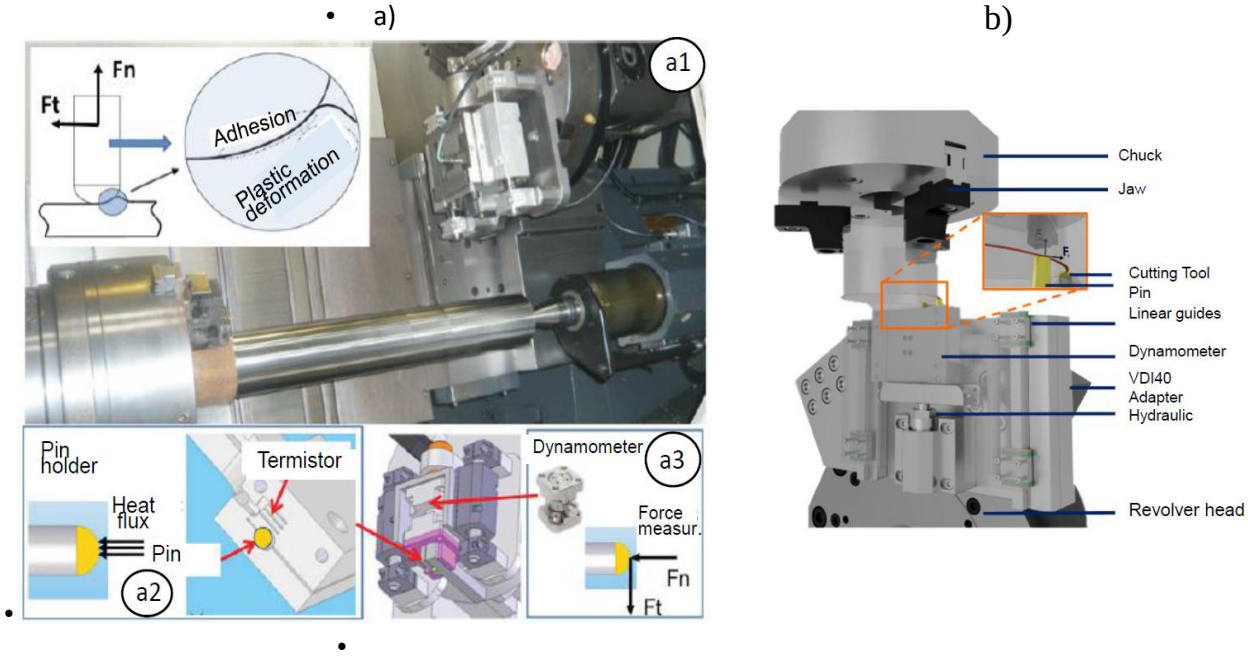

Fig. 1. A scheme of open pin-on-disc tribometer showing local friction conditions in the contact (cutting) zone (a) [3,8], Description: a1- view of working space, a2- temperature and heat flux measurement, a3- measurement of cutting forces and design of the optional open or closed tribometer fitted on vertical lathe center (b) [6]

In the popular open *pin-on-disc* tribometer, a pin holder representing the cutting edge is mounted in a piezoelectric force gauge (Fig. 1a) designed to measure the macroscopic normal (F_n) and tangential (F_t) forces in the contact area. The required normal force is provided by a controlled hydraulic piston (Fig. 1b). As a result, the value of the average (apparent) coefficient of sliding friction, i.e., *the macroscopic coefficient of friction*, is determined as the ratio of these forces:

$$\mu_{app} = \frac{F_t}{F_n} = \frac{F_\gamma}{F_{\gamma N}} \tag{1}$$

In case of a real cutting process the componential forces ($F_{\gamma N}$) and (F_γ) in the directions normal and parallel to the rake face (symbol A_γ according to ISO) are usually measured. It should be mentioned that those measurements are not correct, as they do not care about the ploughing forces of the cutting edge. From the measured forces the ploughing force needs to be subtracted and the remainder split up normal and tangential to the rake face.

Tribometers can be classified as open and closed [3]. The former design simulates the constant feed of fresh material into the contact by placing a cutting insert in front of the pin to machine the workpiece [3]. In conventional closed tribometer, as in pin-on-disc configuration, no cutting insert is used and the pin glides over the old wear track after one revolution of the spindle [6]. An example of the design of optional open or closed tribometer fitted on a turning centre is shown in Fig. 1b, where some aspects of the cutting process are monitored, including the chip formation process and temperature field using a thermal imaging camera [1, 6].

The term "*apparent friction coefficient*" is used because it may differ slightly from the "*interfacial friction coefficient*", which is caused by mechanical interaction (*m*) and adhesion (*a*) at the contact between the pin and the workpiece, as shown in Fig. 1a. The macroscopic forces measured by the tribometer include adhesion phenomena influenced by properties such as hardness, chemical reactivity and roughness, as well as, plastic deformation of the workpiece, which cannot be neglected under the contact conditions induced by this tribometer. The two-term analytical model presented in [1] allows the apparent friction coefficient (μ_{app}) to be extracted as the sum of the mechanical and adhesive components:

$$\mu_{app} = \mu_m + \mu_a \tag{2}$$

where: μ_m – the constant mechanical component, μ_a – the variable adhesive component.
If a thermistor is installed in the spindle (Fig. 1a), the heat flux resulting from friction energy dissipation can be determined. The influence of cutting conditions in conventional and hybrid machining processes on the friction behaviour can be found in the review article [9] and reference [6]. These influences generally include:

- processed material: chemical composition, microstructure,
- tool wedge material: substrate, applied coating, surface micro-texture,
- cooling/lubrication: cooling and lubricating medium, delivery technique.
- contact conditions in the sliding pair.

This study presents the efforts made to verify and possibly update previous friction and process models [4], taking advantage of the significant progress in AI-based techniques.

2. METHODS FOR PREDICTING FRICTION COEFFICIENT VALUES BASED ON TRIBO-TEST DATA

Predicting accurate friction coefficients for various cutting conditions consists of two challenges. While the first challenge is concerned with the identification of friction

coefficients under metal cutting conditions, the second challenge is to mathematically describe the friction behaviour and integrate it into the FEA engine for cutting simulations.

As it is commonly known in the field, applying a constant coefficient of friction does not describe the friction behaviour at the tool correctly. Therefore studies focused on the identification of friction models depending on the local thermo-mechanical loads at the tool. In the experiments conducted by Puls *et al.* [10], a temperature dependent friction model was proposed which incorporates a thermal softening term found in the Johnson-Cook (J-C) flow stress model, which results in a power law to predict the friction coefficient. Several researchers proposed velocity dependent friction models [11]. In a recently published study on friction modelling by Volke et al. [12], an exponential function is used to approximate the dependence of the COF on the sliding velocity. More details are provided by Schulze *et al.* [7].

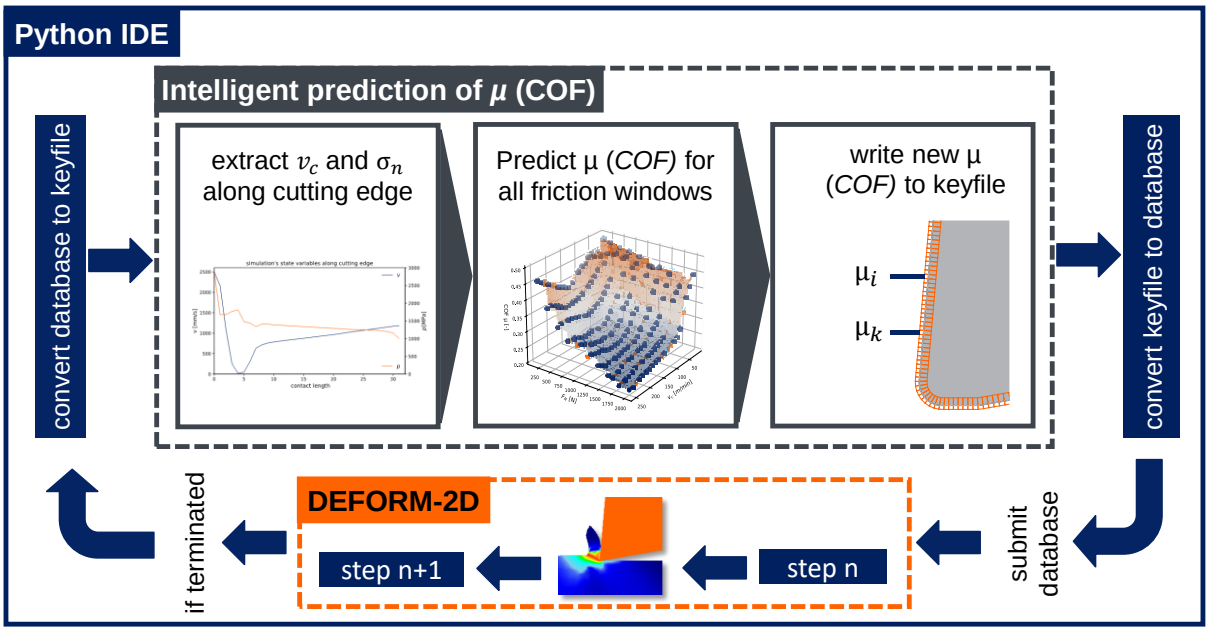

Fig. 2. Python interface enabling data driven input of friction model in FEM DEFORM-2D package [6]

This regression method, often implemented using an exponential function, can become difficult to apply when dealing with high-dimensional inputs, such as temperature, sliding speed, normal pressure, coating wear, and other factors within a single model. In contrast, artificial intelligence techniques are well suited for capturing complex, high-dimensional nonlinear behaviour and can approximate such relationships through regression. The integration of AI into finite element analysis represents a shift toward grey-box modelling, where data-driven intelligence is combined with established physical laws. Nevertheless, despite these advantages, the use of AI to generate predictions within FEA was just recently proposed by Wolf *et al.* [6]. They locally predicted friction coefficients at the tool-chip-interface depending on normal pressure and velocity after conducting pin on disk experiments under differing load and velocity to generate a large dataset. To enable the prediction within the simulation, a unique interface for integrating AI regression approaches was presented, as depicted in Fig. 2 and partially builds on previous works by Wolf *et al.* [13].

By using, for example, a custom Python interface [14], one can achieve local prediction of friction coefficients dependent on sliding velocity and normal pressure along the cutting edge in machining simulations. This allows for direct integration of typical machine learning libraries into the FEM tool. The interface converts databases in FEM-DEFORM package into human-readable text files containing simulation data such as node coordinates, stress, and temperature. Python codes can then modify model parameters, update the number of simulation steps, reconvert the files into DEFORM databases and execute simulations via command line which results in a fully automated workflow. Additionally, DEFORM's friction windows allow specifying local friction laws for tool-chip and tool-workpiece contact. By mapping node positions to these windows and extracting local pressures and sliding velocities, AI models implemented in Python can predict the coefficient of friction, forming a Grey-Box [15] cutting simulation framework without relying on Fortran. In [16], artificial neural networks with the VUHARD subroutine were used to predict the plastic flow stress in the constitutive model defined with Fortran. More information on surface modelling based on artificial intelligence techniques, such as artificial neural networks (ANNs), or other learning methods (ML – *Machine Learning*, DL – *Deep Learning*) is provided in [10].

In [6], a total of four regression models are evaluated: *random forest regression* (RF), *support vector regression* (SVR), extreme *gradient boosting* (XGBoost) and feed forward neural networks (FFNNs). These models were previously discussed in their application to FEM modelling of cutting forces [17,18]. Some characteristic architectures of ML techniques are presented in Fig. 3a and 3b.

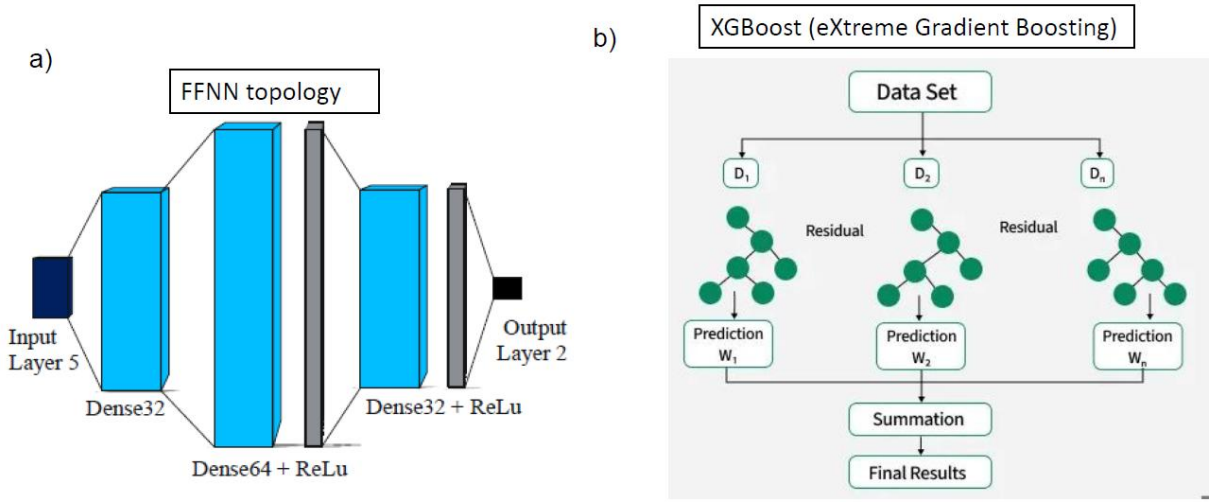

Fig. 3. Exemplary architecture of feed forward neural network (*FFNN*) (a) [19] and extreme *gradient boosting* (XGBoost) [20] (b) Symbols: D – Dataset, W – Weight

Typical topology of a FFNN consisting of three hidden layers, two of which containing dropout layers used in this study are presented in Fig. 3a. In order to guarantee a non-linear functionality the output is sent through an activation function, the rectified linear unit, short ReLU [19]. Manual hyperparameter tuning was performed. Different learning rates, in the range 0.01–0.001, as well as dropout probabilities for both dropout layers were systematically varied (0.3–0.5–0.7). The lowest scores of MAE and MSE metrics were taken for comparison.

XGBoost (eXtreme Gradient Boosting) is a distributed, open-source machine learning library that uses gradient boosted decision trees, a supervised learning boosting algorithm that makes use of gradient descent. It is known for its speed, efficiency and ability to scale well with large datasets [21]. The library is available for C++, Python (Fig. 2), R, Java, Scala and Julia.

To obtain significant information regarding the regression capabilities of the different algorithms, the mean absolute error (MAE), mean square error (MSE), and mean absolute percentage error (MAPE) metrics were calculated. One thousand bootstrap samples were introduced to gain insight into the variability in model performance due to random sampling. *Bootstrap, or so-called self-supporting methods*, are methods for estimating the distribution of estimation errors using multiple sampling with replacement [22].

These algorithms are particularly useful when the distribution of the variable in the population is unknown. The regression coefficient R^2 is given as a point estimate. The learning performance of all four regression models was evaluated using the aforementioned error metrics. Of these, the *XGBoost model* demonstrated the best overall performance, achieving the lowest mean absolute error (MAE = 0.0025), mean square error (MSE ≈ 0.0000), and mean absolute percentage error (MAPE = 0.0078), along with the highest coefficient of determination (R^2 = 0.9913). The Random Forest model also demonstrated high predictive accuracy (MAE = 0.0048 and R^2 = 0.9890). The next best models, the support vector machine (MAE = 0.0090, R^2 = 0.9670) and the FFNN model (MAE = 0.0052, R^2 = 0.9737), also performed well. After calculating the adhesive friction coefficient inversely by FEA, the following raw data Fig. 4a (left) and the result for the XGBoost regression Fig. 4b (right) are determined. Here the test data is of special interest to quantify the metrics above and judge on the models performance. As it can be seen, the predictions on unseen training data are very close to the test data, revealing the strong capability of ML models in complex non-linear regression tasks.

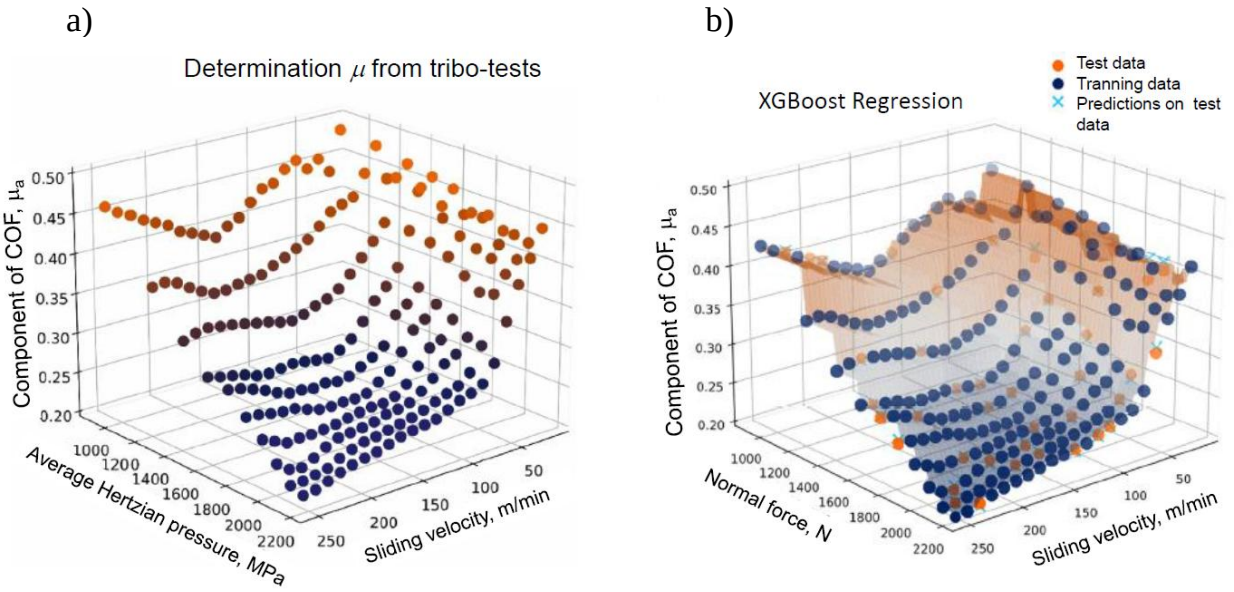

Fig. 4. Measurement results of COF(a) and regression result using XGBoost algorithm (b) [6]

The confidence intervals for the MAPE and MAE metrics were narrowest for XGBoost and Random Forest models, indicating greater stability and robustness of these models. In contrast, FFNNs showed a significantly wider upper bound in its MAPE interval (up to 0.316), suggesting variability in the relative prediction accuracy. Overall, the tree-based ensemble methods (RF and XGBoost) outperformed SV and FFNNs in the training phase, both in terms of point estimates and confidence intervals, highlighting their superior ability to capture hidden data patterns with consistent reliability.

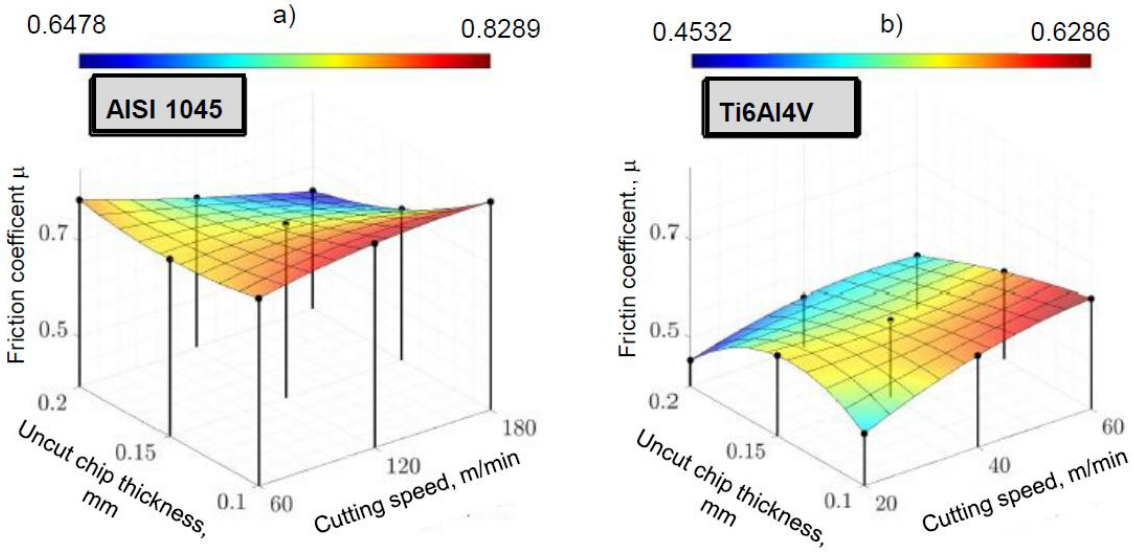

Fig. 5. Dependence of apparent coefficient of friction calculated directly from the measured componential cutting forces (F_p/F_c) on the uncut chip thickness and the cutting speed [17]

It is interesting to compare the test results and the subsequent use of these data for modelling the process using the FEM method and the meshless SPH (*Smoothed Particle Hydrodynamics*) method [23]. The aim of the modelling was to achieve the smallest errors in predicting the values of the cutting force components and temperature using the J-C material constitutive model [1]. Figure 5a and b present the dependence of the friction coefficient value on the undeformed chip thickness (h) and cutting speed (v_c) for non-alloyed AISI 1045 (C45) carbon steel and the two-phase titanium alloy Ti6Al4V, respectively. In this study, AISI 1045 is in a normalized heat treatment condition, which is commonly used for various automotive power-train components with a hardness of 167 HV2, while Ti6Al4V has a hardness of 330 HV2. The following cutting parameters for the machined materials were used in the tests: v_c = 180 m/min and 60 m/min. The tool and cutting edge are characterized by tool material HF-K40 with grain size of 0.6 μm, uncoated, rake angle $\gamma_o = 0^\circ$, clearance angle $\alpha_o = 10^\circ$, cutting edge radius r_β = 10 μm, rake face wet compressed air blasted, average roughness $R_Z = 0.96\ \mu m$. Three thicknesses of the removed material layer were used: h = 0.1, 0.15 and 0.20 mm [17]. Figure 5 shows significant differences in the COF (μ) value, which are caused by the higher temperature measured at the chip-tool contact and the effect of thermal softening of the difficult-to-cut titanium alloy [1]. The average value of the friction coefficient $\bar{\mu} = 0{,}738$ for AISI 1045 steel was determined to be 40% higher than for the Ti6Al4V titanium alloy for which $\bar{\mu} = 0{,}541$. The maximum values were determined for the smallest thickness

of the removed layer, which corresponds to the highest specific cutting energy (documented in [1]) and the highest cutting speed.

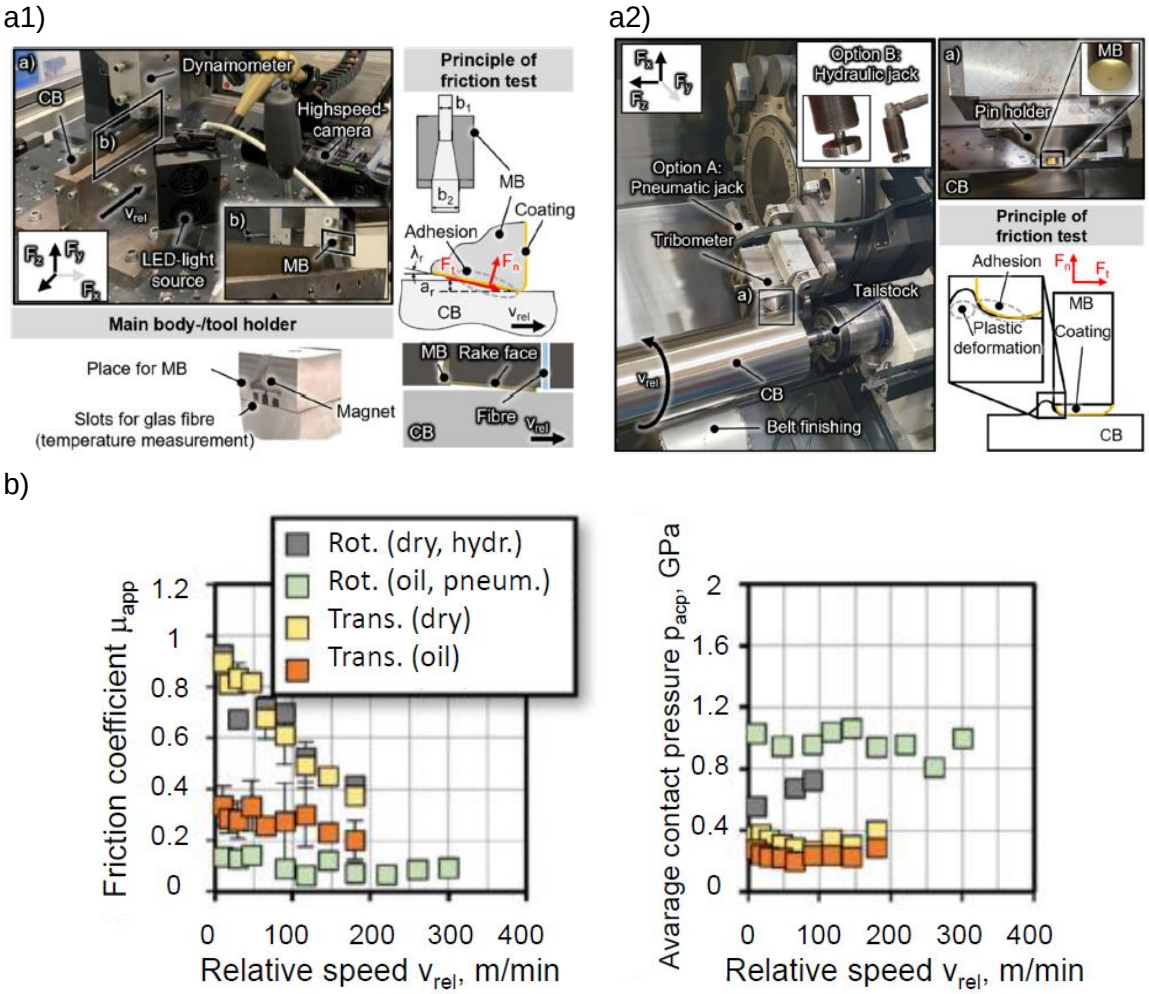

Fig. 6. Experimental set-up used in friction characterization under translation (a1) and rotational (a2) relative movement and some outputs (c) showing the influence of relative speed on the apparent friction coefficient and apparent contact pressure [5] Conditions: AISI 316L steel *vs* TiN coated WC, symbols: MB- main body, CB- counter body

Friction tests covering both rotational (typically in turning operations) and translational (typically in plane operations) relative movements (Fig. 6a1 and a2) were carried out as a French-German collaborative project under different cooling-lubricating conditions and different cutting tool preparation [5]. Some results of this comparative study are presented in Fig. 6b. The figure shows that the changes in the friction coefficient with the relative speed for the dry condition agree very well for the rotational and transitional relative motions. The high apparent coefficients of friction that were previously reported in [24] in the dry state at low relative speeds, were confirmed by both experimental setups and can be attributed to the adhesive material behaviour of AISI 316L corrosion-resistant steel. The tendency of decreasing friction coefficients with increased cutting speed in both experimental setups (higher for dry conditions) can be attributed to the comparable average contact pressures applied (see right figure), leading to similar friction coefficients and, consequently, similar dissipated friction power.

3. FEM MODELLING USING EXPERIMENTALLY AND AI-BASED GENERATED FRICTION DATA

In Fig. 7, cutting force (F_c) and passive force (F_p) for the two materials are shown depending on the cutting speed. Measured values are compared to the simulated values for different functional models for the friction coefficient and different discretisation methods (SPH and FEM). It shows that in general the constant characteristic values for the COF values μ = 0.76 and 0.56 for AISI 1045 and Ti6Al4V respectively based on the data from Fig. 5 do represent the situation fairly well, while the functional dependencies of COF on the cutting speed and the temperature cannot enhance the prediction significantly.

The prediction errors of the average forces using the FEM and SPH methods are in the range of 33% to 23%. Except for the temperature on the rake face of the titanium alloy, the temperature predictions were found to be more accurate – in the range of 5–20% [17].

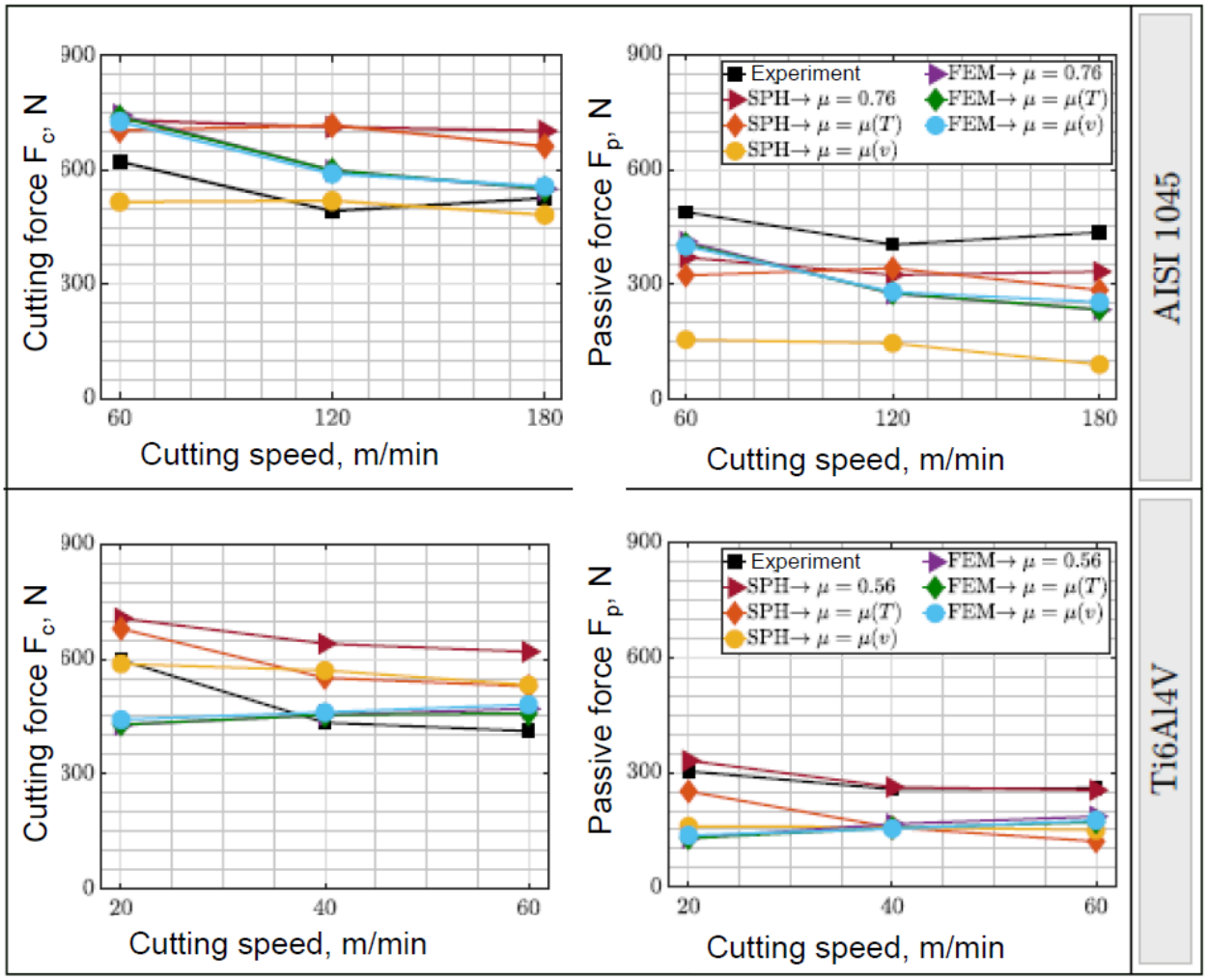

Fig. 7. Comparison of measured and predicted cutting forces at different cutting speeds and COF modelling methods (constant h = 0.10 mm) [17]

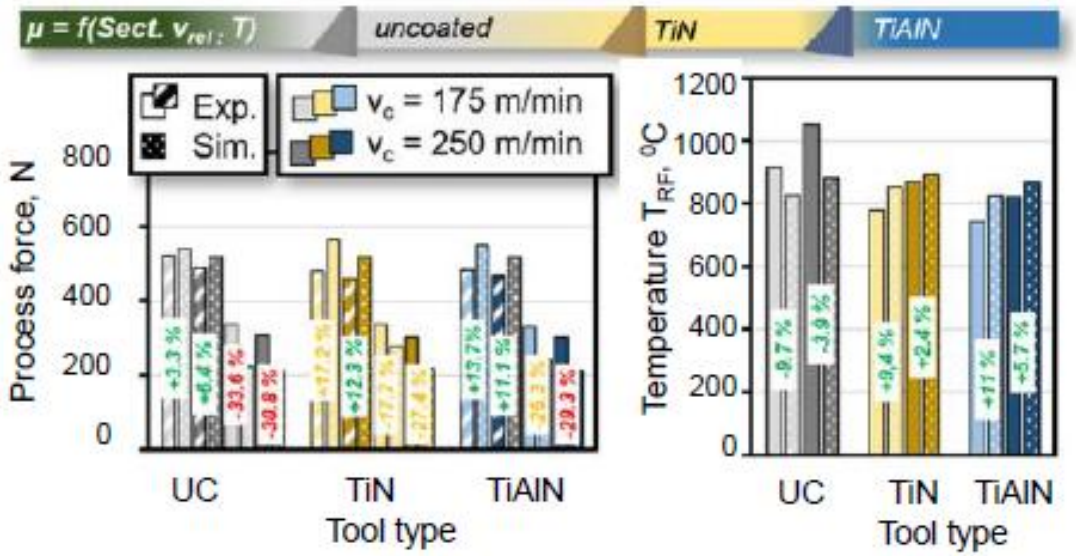

Fig. 8. Results of FEM simulation (DEFORM 2D) of chip formation showing variations of coating deposition using the sectional relative speed and temperature-dependent friction model [5]. Conditions: AISI316L steel *vs* UC, TiN and TiAlN coated WC, cutting speed v_c = 175 and 250 m/min, uncut chip thickness h=0.1 mm, dry

Parameters of the friction law, independent of whether a coulomb law or stress-speed and/or temperature dependent friction models are used, are as uncertain as the parameters of the constitutive model of the workpiece material used. Due to the extreme conditions in the cutting zone, even a split Hopkinson bar test is incapable to provide sufficient shear stress rates, which means that the parameter identification needs to be performed in an orthogonal cutting test. Here, the friction law needs to be considered as an additional constitutive law and its parameters identified in the same orthogonal cutting test. Tribo-tests from tribometers creating a friction zone similar to cutting process like explained in Ref. [30] might be used as starting or reference value for the identification procedure. As this method requires a larger number of computation test run, overall computational efficiency becomes crucial which makes the highly parallelizable SPH discretization method, the method of choice. A contribution to this approach can be found in [17, 25]. This research clearly shows that the modelling of the friction law is insufficient to compensate defects of the J-C material's constitutive law.

The results of FEM simulation (DEFORM 2D) of chip formation for different coating deposition (UC, TiN, TiAlN) using the sectional relative speed and temperature-dependent friction models, (μ = f(v_{rel})) and (μ = f(T)), respectively, are shown in Fig. 8 [5]. It can be seen that the accurate prediction of the cutting force also enables precise prediction of the temperature field within the contact area on the rake face. The mean deviation from experimentally determined rake face temperatures for uncoated, TiN and TiAlN-coated tools is ΔTRF = +2.5% across both cutting speeds. In the sectional friction model, on the other hand, the temperatures are already overestimated by ΔTRF= + 10.1%. Therefore, it can be assumed that the temperature dependent friction model will be more accurate with longer cutting paths up to the thermal steady state. This observation is consistent with the results reported in Ref. [17], where both FEM and SPH models and the friction models (μ_T) and (μ_v) were used, as shown in Fig. 7.

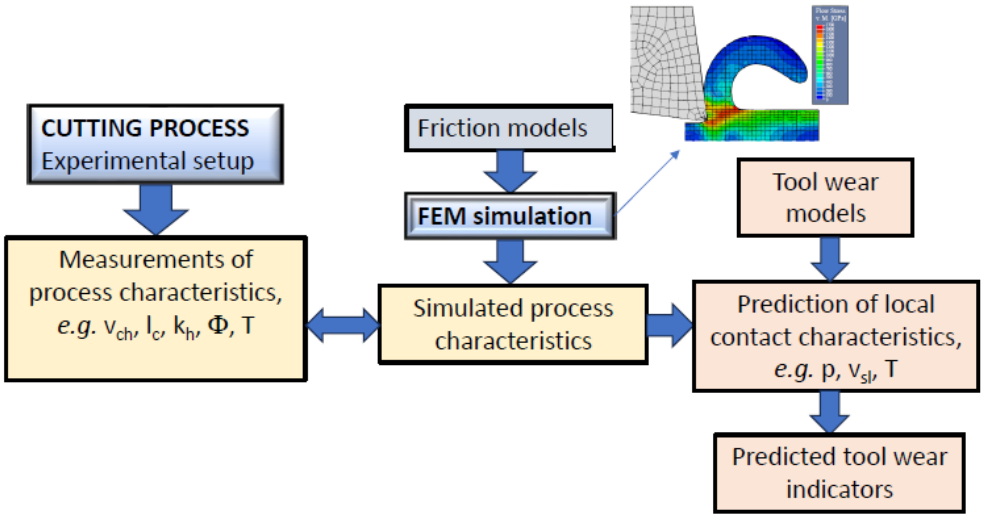

Fig. 9. Flowchart for determining the effects of the friction model type on the tool wear. Adapted from [18]

Figure 9 shows a methodology of tool wear prediction using four different friction models, in an integrated manner as input to DEFORM FEM simulation. Examples of these friction models are Zorev's *shear friction* model (SFM), Coulomb *friction model* given by the relationship $\tau_f=\mu\sigma_n$ (CFM), *hybrid friction model* (HFM) using a shear friction factor *m* and the shear flow stress *k* ($\tau = mk$), and the constant *tau* (τ) *model* (CTM) [1, 4, 18]. The CTM is obsolete in continuum mechanical simulations, because the constitutive equations alone give the correct shear limit of the material including work hardening. In addition, some important thermo-mechanical process characteristics, including the contact length, the chip compression ratio, the shear angle and the cutting temperature are predicted using the J-C constitutive material model.

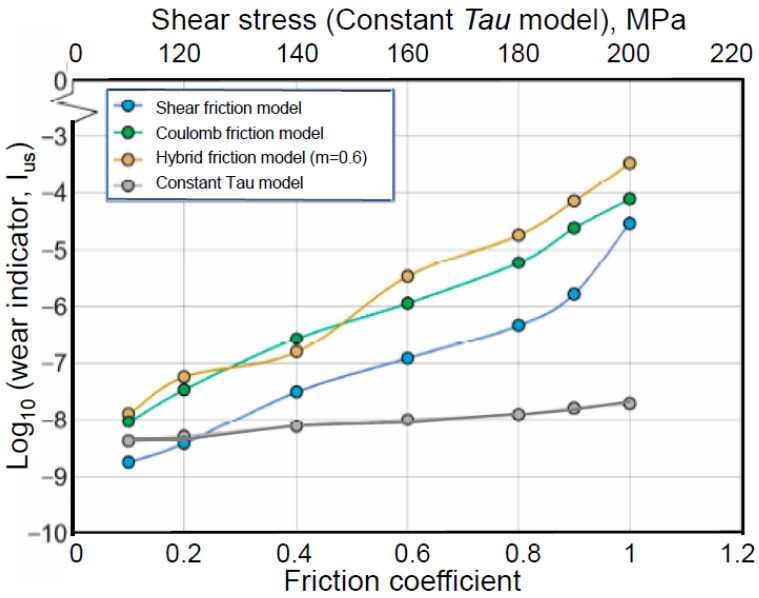

Fig. 10. Effects of friction coefficient and the shear stress along the cutting edge on wear indicator using Usui's wear model [1, 18]

In general, tool wear can be determined analytically by the Archard's or Usui's models [1] (see Fig. 10). Usui's model that considers predominantly attrition following by adhesive wear is given by Eqn. (3a) [1].

$$\frac{dW}{dt} = C_1\,\sigma_n v_s \exp\left(-\frac{C_2}{\theta}\right) \tag{3a}$$

where: σ_n – the normal stress, v_s – the relative sliding velocity, θ – the interfacial temperature and C_1 and C_2 are constants.

Consequently, the tool wear (I_{Us}) can be estimated using the logarithmic form of Usui's model (3a), with $\log_{10}(I_{Us})$ is given by Eqn. (3b) [15].

$$\log_{10}(I_{Us}) = \log_{10}\left(\sigma_n\, v_s\, e^{-\frac{E}{RT}}\right) \tag{3b}$$

where: E – the process activation energy, R – the universal gas constant, T – the absolute thermodynamic temperature at the tool-chip contact.

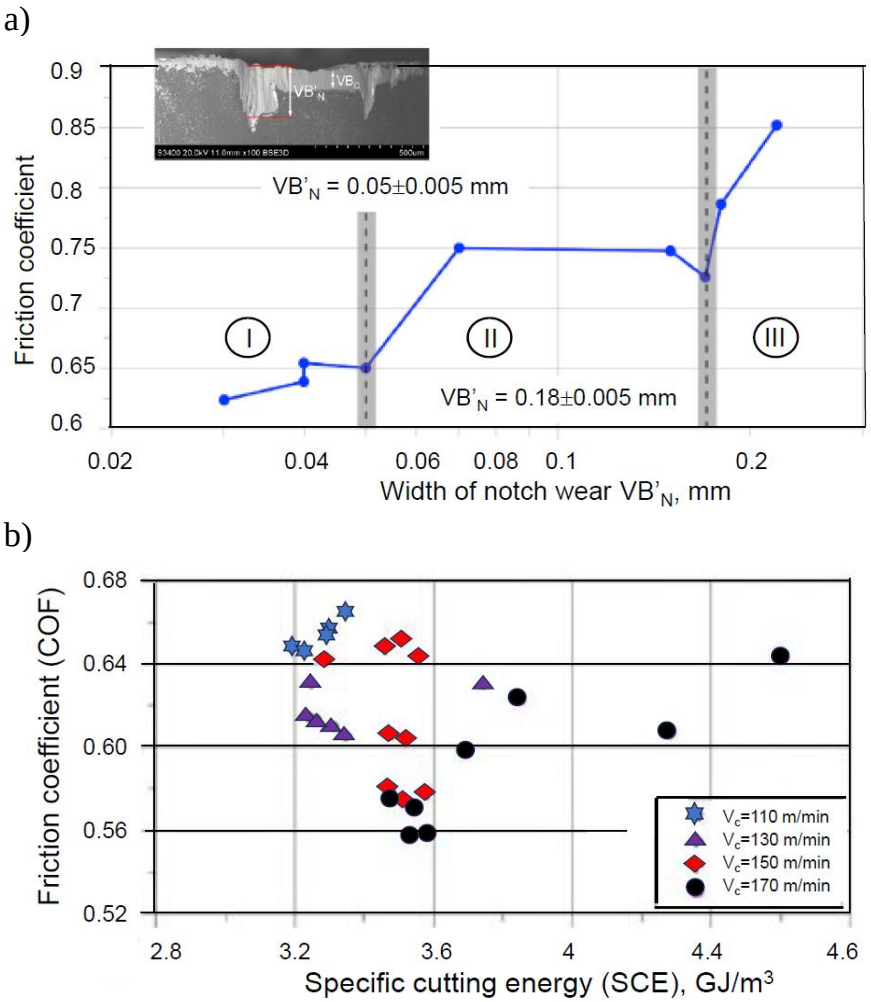

Fig. 11. The dependence of the friction coefficient on tool wear state. Work material- Inconel 718, tool material: PVD-AlTiN coated WC-Co, cutting parameters: v_c = 80 m/min, a_p = 0.25 mm, f = 0.1 mm). (a) [20] and the specific cutting energy, Work material: Ti6Al4V alloy, tool material: PVD-AlTiN coated WC-Co (b) [28]

Using Eqn. (3b), the dependence of tool wear on the friction model type can be determined as illustrated in Fig. 10. The figure shows the effect of the friction coefficient μ and shear stress τ_c at the tool-chip contact on the Usui's wear indicator $\log_{10}(I_{Us})$. It can be seen that an increase in the friction coefficient μ and shear stress at the tool-chip contact results in an increase in the predicted tool wear.

It can also be observed in Fig. 10 that the degree of wear increase is approximately the same for the CFM and HFM models, and partially for SFM friction model, with the highest wear expected when using the HFM model with *m* factor equal to 0.6. It can be noted that higher wear indicators coincide well with the higher values of COF resulting probably from adhesive interaction between the tool and the chip. The presence of an intensive adhesive wear was documented in friction test provided in Refs. [6,15].

It was documented in Ref. [26] that such cutting characteristics as the cutting force, the specific cutting energy (SCE) and friction coefficient change during tool wear represented by the three characteristic periods distinguished in Fig. 11a. They cover the measured values of notch wear (VB'_N) from 0 to 0.05 mm (period I), 0.05–0.18 mm (period II) and 0.18–0.22 mm (period III). Consequently, as shown in Fig. 11a, three characteristic tool wear periods depicted in the Lorentz'wear curve [1], i.e. running-in (I), uniform (II) and accelerated/catastrophic (III) correspond to the characteristic values of COF. In the second period the coating is locally removed and the friction coefficient increases up to $\mu = 0.75$ due to adhesive interactions caused by the transferred Inconel 718 [23,27]. In addition, this process coincidence in relation not only to the SCE but also to the contact temperature and the thermal diffusivity was depicted for Ti6Al4V alloy versus AlTiN coating as shown in Fig. 11b. Cutting tests were performed for different cutting speeds and the cutting length of about 1250 m, and constant cutting parameters: a_p = 0.25 mm; f = 0.1 mm/rev [28]. As shown in Fig. 11b, friction coefficient is correlated with the SCE values and is sensitive to tool wear progress, which, in turn, causes relevant increase of the SCE. In this study (Fig. 11b) the friction coefficient changes in the range of 0.56–0.66 after the cutting (sliding) distance of about 1250 m. It can be seen that the COF values determined in this study correspond to those predicted by FEM simulation in [17]. The above-mentioned correlations of COF with process characteristics suggest a multiple approach to modelling and AI-based prediction of COF values, which correspond more accurately with the process performance and measured outputs.

4. SUMMARY

Cutting process modelling can be based not only on well-known numerical methods such as FEM and SPH, but also supported by intelligent regression algorithms (e.g., extreme gradient boosting (XGBoost)) and neural networks (e.g., FFNNs with back propagation) with learning capabilities to accurately predict input data, including the friction coefficient. Tribo-tests combined with measurements of component forces and temperature, or tool wear, play an important role in experimental studies that are the basis for model validation. It has been shown that in some cases, meshless SPH modelling provides more accurate predictions of cutting process characteristics [17]. In order to achieve better agreement between

measurement data and simulations, various friction models can be introduced into the FEM package, e.g. DEFORM [18], in an integrated manner, e.g. shear friction model (SFM), Coulomb friction model (CFM), hybrid friction model (HFM), constant tau model (CTM). Using these friction models and taking into account the corresponding COF values the tool wear rate can be predicted. The highest wear rates were obtained when using HFM model with given value of the *m* factor. Finally, it can be reasoned that the complexity of friction and wear predictions needs the integration of experimental and modelling tasks possibly with appropriate machine learning algorithms and AI-assistance. It is very likely, that this trend will be developed in the future machining research with focus on high performance machining [29].

ACKNOWLEDGEMENTS

This paper is dedicated to the memory of our Esteemed CIRP colleague prof. J. Jedrzejewski who was not only for three decades the editor-in-chief for the Journal of Machine Engineering but predominantly an excellent scientific mentor and organizer of the world-famous series of CIRP-sponsored conferences held in Karpacz, Poland. Authors are very thankful to prof. H.-Ch. Möhring from University of Stuttgart, Germany for his valuable contribution and comments.

REFERENCES

[1] GRZESIK W., 2017, *Advanced Machining Processes of Metallic Materials*, Elsevier.
[2] RECH J., CLAUDIN CH., POLLY P., COURBON C., 2016, *New Aspects of Metrology of Frictional Behavior in Metal Cutting*, Mechanik, 11, 1751–1753, DOI: 10.17814/mechanik.2016.11.520.
[3] GRZESIK W., RECH J., 2019, *Development of Tribo-Testers for Predicting Metal Cutting Friction*, Journal of Machine Engineering, 19/1, 62-70.
[4] MELKOTE S.N., GRZESIK W., OUTEIRO J., RECH J., SCHULZE V., ATTIA H., ARRAZOLA P.J., M'SAOUBI R., SALDANA CH., 2017, *Advances in Material and Friction Data for Modeling of Metal Machining*, CIRP Annals, 66/2, 731–754, https://doi.org/10.1016/j.cirp.2017.05.002.
[5] VOLKE P., COURBON C., KRUMME E., SÄLZER J., RECH J., BIERMANN D., 2024, *Frictional behaviour of coated carbide tools and AISI 316L when using translational and rotatory relative movement considering dry and lubricated conditions*, CIRP Journal of Manufacturing Science and Technology, 51, 36–46, https://doi.org/10.1016/j.cirpj.2024.03.011.
[6] WOLF A., BANDARU N.K., DIENWIEBEL M., MÖHRING H.-CH., 2025, *A Novel Grey-Box Based Friction Model for a Wide Range of Machining Conditions*, Wear, 580–581:206295, DOI: 10.1016/j.wear.2025.206295.
[7] SCHULZE V., BLEICHER F., COURBON C., GERSTENMEYER M., MEIER L., PHILIPP J., RECH J., SCHNEIDER J., SEGEBADE E., STEININGER A., WEGENER K., 2022, *Determination Of Constitutive Friction Laws Appropriate For Simulation Of Cutting Processes*, CIRP Journal of Manufacturing Science and Technology, 38, 139–158, https://doi.org/10.1016/j.cirpj.2022.04.008.
[8] GRZESIK W., 2026, *Advanced Methods of Determination of Friction Coefficient in The Machining Process*, Mechanik, 1, 8–13, DOI: https://doi.org/10.17814/mechanik.2026.1.1.
[9] GRZESIK W., RECH J., 2019, *Influence of Machining Conditions on Friction in Metal Cutting Process - a Review*, Mechanik, 4, 242–248, DOI: https://doi.org/10.17814/mechanik.2019.4.33.
[10] PULS H., KLOCKE F., LUNG D., 2014, *Experimental Investigation on Friction Under Metal Cutting Conditions*, Wear 310, 63–71, https://doi.org/10.1016/j.wear.2013.12.020.
[11] SMOLENICKI D., BOOS J., KUSTER F., ROELOFS H., WYEN C.F., 2014, *In-Process Measurement of Friction Coefficient in Orthogonal Cutting*, CIRP Annals – Manufacturing Technology, 63, 97–100, https://doi.org/10.1016/j.cirp.2014.03.083.
[12] VOLKE P., COURBON C., KRUMME E., SAELZER J., BIERMANN D., 2024, *Frictional Behaviour of Coated Carbide Tools and AISI 316L when Using Translational and Rotatory Relative Movement Considering Dry and*

Lubricated Conditions, CIRP Journal of Manufacturing Science and Technology, 51, 36–46, https://doi.org/10.1016/j.cirpj.2024.03.011.
[13] WOLF J., REEBER T., BANDARU N.K., DIENWIEBEL M., MÖHRING H.-CH., 2024, *Transient Wear modelling of Coated Cutting Tools*, Procedia CIRP, 130, 1827–1831, https://doi.org/10.1016/j.procir.2024.10.323.
[14] Python Interface, (online, accessed: 18/01/2026),
[15] *What Is Grey-Box Testing?*, (online, accessed: 18/01/2026), https://www.imperva.com/learn/application-security/gray-box-testing/.
[16] DUCOBU F., PANTALÉ O., LAUWERS B., 2024, *Predictive 3D Modeling of Free Oblique Cutting Introducing an ANN-Based Material Flow Law with Experimental Validation Over a Wide Range of Conditions*, Int. J. Adv. Manuf. Technol., 131, 921–934, https://doi.org/10.1007/s00170-024-12956-7.
[17] AFRASIABI M., SÄLZER J., BERGER S., IOVKOV I., KLIPPEL H., RÖTHLIN M., ZABEL A., BIERMANN D., WEGENER K., 2021, *A Numerical-Experimental Study on Orthogonal Cutting of AISI 1045 Steel and Ti6Al4V Alloy: SPH and FEM Modeling with Newly Identified Friction Coefficients*, Metals, 11, 1683. https://doi.org/10.3390/met11111683.
[18] STORCHAK M., MELNYK O., STEPCHYN Y., SHYSHKOVA O., GOLUBOVSKYI A., VOZNIY O., 2025, *Effect of Friction Model Type on Tool Wear Prediction in Machining*, Machines, 13/10, 904, https://doi.org/10.3390/machines13100904.
[19] REEBER T., WOLF J., MÖHRING H.-CH., 2024, *A Data-Driven Approach for Cutting Force Prediction in FEM Machining Simulations Using Gradient Boosted Machines*, J. Manuf. Mater. Process., 8, 107, https://doi.org/10.3390/jmmp8030107.
[20] Implementation of XGBoost (eXtreme Gradient Boosting), (online, accessed: 18/01/2026), https://www.geeksforgeeks.org/machine-learning/implementation-of-xgboost-extreme-gradient-boosting/.
[21] GRZESIK W., RUSZAJ A., 2021, *Hybrid Manufacturing Processes. Physical Fundamentals, Modelling and Rational Applications*, Springer Nature Switzerland AG.
[22] Bootstrap (statistics), (online, accessed: 18/01/2026), https://pl.wikipedia.org/wiki/Bootstrap_(statitistics).
[23] GRZESIK W., 2024, *Progress in Modeling and Simulation of the Machining Process – Part II: Mesh-Free Modeling and Simulation*, Mechanik, 4, https://doi.org/10.17814/mechanik.2024.4.6.
[24] VALIORGUE F., RECH J., HAMDI H., BONNET C., GILLES P., BERGHEAU J.M., 2008, *Modelling of Friction Phenomena in Material Removal Processes*. J. Mater. Process. Technol., 201,1–33, 450–453.
[25] ZHANG N., KLIPPEL H., KNEUBÜHLER F., AFRASIABI M., KUFFA M., WEGENER K., 2024, *Investigation of Friction Modeling on Numerical Ti6Al4V Cutting Simulations*, Int. Journal of Mechanical Sciences, 274, 109231.
[26] GRZESIK W., ZAK K., ZAWADA-TOMKIEWICZ A., 2024, *Analysis and Modelling of Surfaces Produced by Subtractive Machining*, PWN, Warsaw.
[27] GRZESIK W., NIESLONY P., HABRAT W., SIENIAWSKI J., LASKOWSKI P., 2018, *Investigation of Tool Wear in the Turning Of Inconel 718 Superalloy In Terms of Process Performance and Productivity Enhancement*, Tribology International, 118, 337–346, https://doi.org/10.1016/j.triboint.2017.10.005
[28] GRZESIK W., NIESLONY P., HABRAT W., 2019, *Investigation of the Tribological Performance of Altin Coated Cutting Tools in the Machining Of Ti6Al4V Titanium Alloy in Terms Of Demanded Tool Life*, Maintenance and Reliability, 21/1, 153–158, http://dx.doi.org/10.17531/ein.2019.1.17.
[29] ULLRICH K., VON ELLING M., GUTZEIT K., DIX M., WEIGOLD M., AURICH J.C., WERTHEIM R., JAWAHIR I.S., GHADBEIGI H., 2024, *AI-based optimisation of total machining performance: A review*, J. of Manufacturing Science and Technology, 50, 40–54, https://doi.org/10.1016/j.cirpj.2024.01.012 .